J Mater Sci (2016) 51:1165–1175
DOI 10.1007/s10853-015-9479-x

INVITED VIEWPOINT

Viewpoint: metallurgical aspects of powder bed metal additive manufacturing

Rainer J. Hebert[1]

Received: 17 July 2015 / Accepted: 5 October 2015 / Published online: 18 November 2015

Abstract Metal additive manufacturing has emerged as a new manufacturing option for aerospace and biomedical applications. The many challenges that surround this new manufacturing technology fall into several different categories. The paper addresses one of these categories, the physical mechanisms that control the additive manufacturing process. Physical mechanisms control the effects of processing parameters on microstructures and properties of additively manufactured parts. Some mechanisms might not have been recognized, yet, and for those that are currently known, detailed quantitative predictions have to be established. The physical mechanisms of metal additive manufacturing are firmly grounded in metallurgy, branching into laser physics and the physics of granular materials. Powder bed additive manufacturing is described from the powder storage to post-processing and elements of metallurgy are highlighted that are relevant for the different aspects of the additive manufacturing process. These elements include the surface reactions on powder particles, the heating and melting behavior of the powder bed, solidification, and post-processing. This overview of the different metallurgical aspects to additive manufacturing is intended to help guide research efforts and it will also serve as a snapshot of the current understanding of powder bed additive manufacturing.

✉ Rainer J. Hebert
rainer.hebert@uconn.edu

[1] Department of Materials Science and Engineering, Institute of Materials Science, Additive Manufacturing Innovation Center, University of Connecticut, 97 N. Eagleville Rd, Storrs, CT 06269, USA

Introduction

Much fanfare has surrounded 3-D printing recently and products with revolutionary new designs should be available very soon. The excitement about 3D-printing of plastic materials originates mainly from a combination of low-cost 3D printing machines, enabling students and hobbyists to design and make plastic parts, and from specific industry uses such as biomedical implant components. While polymeric materials have for a long time dominated 3D-printing, metals have recently made strong inroads [1]. The interest stems mostly from the ability to manufacture parts without the need for tooling and therefore with reductions in lead time and tooling cost. The ability to manufacture parts directly from powder is very advantageous for those legacy components for which tooling and fixtures no longer exist. In these situations, when only a few parts of a particular design are needed, the cost of tooling often proves prohibitive in producing the replacement parts. Additive manufacturing furthermore promises advances in situations when large inventories of parts cannot be maintained, for example, in mobile military applications or in space applications. In these situations, "on-demand" manufacturing based on the small footprint that additive manufacturing affords, even including necessary post-processing operations, can potentially change the ability for forward projection. Another advantage of metal additive manufacturing is the reduced raw material need in cases when traditional manufacturing involves high percentages of scrap production. The layer-by-layer manufacturing approach furthermore offers some specific advantages for part qualification over conventional techniques such as castings: at least in principal, it should be possible to detect defects in parts during the manufacturing process, reducing the need for post-inspection for qualification purposes.

Another currently largely unused potential of the layer-by-layer technology is the ability to digitally store the processing conditions as a function of position in the part. This information could be sent along in the downstream process of the parts as a detailed part pedigree.

Despite these great promises and many opportunities for metal additive manufacturing on the design side, there are challenges that need to be overcome before the promises and opportunities can become reality. The challenges occur at various levels, starting with the design aspect of additive manufacturing parts as well as the manufacturing side, including a wide array of topics such as process variations, vendor qualifications, part qualifications, or standards, to name only a few. Arguably the most important challenge for production level additive manufacturing is the variations in part properties. These variations can occur on the dimension side or the mechanical property side. In one common approach, a design of experiments (DOE) technique is used to analyze the influence of input parameters such as machine- or material parameters on response variables [2]. In another approach, the machine parameters are mapped to microstructures using thermal- and materials models [3]. A different approach is based on the physical mechanisms that link the input space—machine and material properties—to microstructures and properties of the finished parts. The physical mechanisms that occur during the metal additive manufacturing process comprise a large array of complex metallurgical problems. In the following, the powder bed additive manufacturing process is summarized and its main metallurgical topics are highlighted. This summary of the powder bed process is intended to link the process to metallurgical topic areas and to define potential directions for mechanism-driven process modeling and simulations.

Powder bed additive manufacturing: processing overview

Powder material considerations

Currently, typical powder particle sizes for commercial additive manufacturing machines are in the range of about ten to around 130 micrometers, with wide variations in the specific size distribution, depending on the supplier and also the machine and material selection. For those machines using a raking process to spread powder, the powder shape needs to be spherical in order to facilitate powder flow on the build plates, but for other powder spreading options, for example, rolling, non-spherical powders can be used. The atmosphere in the storage bins and even more so within the additive manufacturing machines during processing has an impact on the surface condition of the powder particles, which in turn might impact not only the effective densities and the powder flow behavior, but also the chemical composition of the melt pool.

For reactive powder materials such as titanium-based or aluminum-based powders, oxide layers form under all but the most severe vacuum conditions, which cannot be achieved with either an argon flow or with the vacuum levels of about 10^{-5} mbar that can be found in electron beam equipment. The Ellingham diagram can be used to determine the partial oxygen pressure conditions that suffice to prevent the formation of oxide layers as a function of temperature [4, 5]. Much more detailed theories, including kinetic considerations, are available, since the topic of oxide layer formation represents a longstanding research topic that has received much interest, although not necessarily for powders [6, 7].

Aside from the formation of oxide layers, the adsorption of water on the powder particle surfaces must be considered [8, 9]. Adsorbed water films impact the powder flow behavior [10] and can modify the melt pool chemistry. The role of water films adsorbed on metal surfaces, in particular on a titanium alloy surface, is documented in publications on electron beam welding [11, 12]. When an electron beam impinges on a surface water film, water molecules can desorb and dissociate. Hydrogen can then enter the melt pool and, depending on the solubility of hydrogen gas in the liquid alloy as a function of temperature, can cause the formation of bubbles that might freeze in or dissolve in the base alloy upon freezing. In the context of powder flow and effective density, adsorbed water films can negatively impact the flow behavior of the powder beds [10, 13, 14]. Besides oxides on the powder particle surfaces, the formation of hydroxides and hydrated oxides should be considered. While oxide layers tend to be hard and brittle, hydroxide layers can assume a gel-like consistency with lubricating effects; these changes in the surface phases profoundly affect the wear behavior of metals [15]. It should be expected that the surface reactions and formation of hydroxides, as opposed to oxides, would also affect the flow of powders and possibly their agglomeration behavior. If the water vapor pressure decreases or the temperature increases, the hydroxides can dry out and crystallize to form oxides and, in the process, change the flow behavior of the powders. The water coming off the hydroxides or hydrated oxides at increasing temperatures could moreover contaminate the atmosphere in the additive manufacturing build chambers or interact with the laser or electron beam. The oxide, hydroxide, hydrated oxide, and water vapor formation represent complex processes that are likely to be interrelated. General theories only exist for specific aspects, for example, the adsorption of water vapor, the oxidation behavior on metal surfaces, or the solubility of gases in solids and liquids. Cause–effect relations for the

powder flow dependence on oxide and water film characteristics are currently only available for specific systems as a result of detailed but individual studies. The limited understanding of the complex relations between alloy composition, temperature, relative humidity, nature of the oxide coverage, and the effects of these parameters on the powder bed response to laser or electron beam melting and the powder flow behavior motivates a key question: how much variation can be expected in the final outcome, i.e., the additively manufactured parts and their properties at the current level of atmosphere control for the powder materials. The changes in the powder flow behavior or the impact on the melting and solidification with variations in the humidity and temperature and hence in the oxide and water film coverage might be too small to control the variations in the properties of additively manufactured parts, or they could turn out to be critical. The answer to this question impacts powder storage. Practical options range from powder handling at all times in an inert atmosphere under low humidity levels, to uncontrolled powder storage conditions. Additional safety aspects play a role in case of flammable powders. If dry storage conditions would turn out to be necessary, an increased risk of electrostatic charging and subsequent spark formation would have to be taken into account.

Powder delivery considerations

Powder bed machines require powder to be loaded into storage compartments. The storage compartments can be hoppers or bins within the machines or can be bins that are attached externally, in closed-loop contact with the machine interiors. From a viewpoint of manufacturing and process control, one important aspect is the exposure of powder to the laboratory environment. In those instances when machines have to be opened for the removal of parts in a way that the powder storage compartments or bins are directly exposed to the lab environment, reactions can take place between the powder and the environment. Contaminants in form of dust or other unwanted particles could enter the machine interior and powder storage if precautions are not taken. The powder is then spread on build plates that are typically steel plates and serve as the basis for building parts. The powder spreading process on the build plates should yield a uniform distribution of powder particles on the plate. "Uniform" in the context of powder spreading over the build plates can be regarded as powder having the same powder size and shape distribution, the same packing density and flow behavior, and the same height everywhere on the build plate. The storage and flow of powder onto the build plate falls at least partially into the realm of granular material physics. The currently available additive manufacturing machines differ in the details of the powder delivery on the build plates with raking, rolling/raking, or gravitational feeding as the most common delivery approaches. How these different approaches affect the uniformity of the powder bed is currently not examined very well. In general, during flow of granular materials, the size distributions might not remain uniform and size-demixing might occur [16, 17]. Changes in the powder size distribution homogeneity could occur both laterally, i.e., in the within the build plate area, and also in the direction of the beam. The powder bed thicknesses are only on the order of approximately 100 micrometers, and therefore, changes in size distributions in the direction parallel to the beams are confined to a few particles. Modeling efforts are currently underway to better understand the beam–powder interactions and it is therefore not yet entirely clear how fluctuations in local effective densities or size distributions in the powder beds affect their melting behavior and the formation of pores. Granular materials science aspects not only play a role for the spreading of powder beds, but should also apply to the storage of the powders in the bins and the recycling process. The storage time and storage conditions can be expected to affect the packing density in the storage bins or compartments and hence the subsequent flow onto the build plate. Sieving strategies are necessary to ensure uniformity of powder beds in the storage compartments within the machines. In some machines, the powder is recycled automatically, in closed-loop processes, and the uniformity of the powder size distributions during the recycle process needs to be tested.

Much of the relation between the powder storage, spreading onto the build plates, and the defect and microstructure formation is hypothetical or anecdotal at best at this point and requires further investigations with controlled experiments. The underlying theme of process variations also applies to the powder spreading aspect. At present, no clear understanding exists of the relations between the storage conditions in the storage compartments, the specifics of the powder spreading, and the uniformity on the build plate. But it is equally if not more important to understand how variations in the storage conditions and powder storage and spreading details affect the uniformity variations on the build plate or the impact that uniformity variations have on the melting and solidification process. Along the same lines, with continued reuse of the powder material, changes occur in composition, size distribution, and surface characteristics of the powder particles [18] that should affect the behavior of the powder during the spreading on the build plates and during the interactions with the laser or electron beams. The processing parameters that affect the powder spreading on the build plates are summarized schematically in Fig. 1. Aside from the powder material itself, the particular

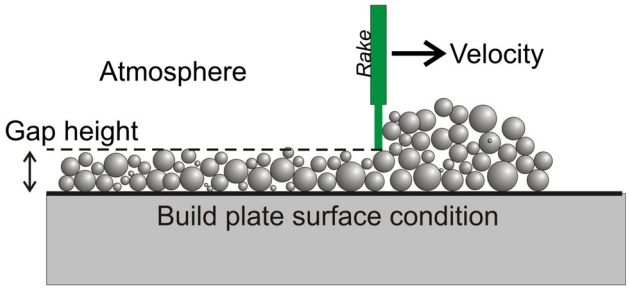

Fig. 1 Schematic illustration of processing parameters for the powder raking process. The rake material and shape, the rake velocity, the gap height from the build plate, the atmosphere, and the surface condition of the build plate should all affect the spreading of the powder bed on the plate

geometry and nature of the rake or roller (only a rake is illustrated in Fig. 1), the atmosphere, the gap height, the rake velocity, and the surface condition of the build plate should all affect the motion of the powder particles during the raking process and should hence affect the powder bed nature.

The metallurgical topics relevant to the broad topic of powder storage and delivery fall mostly into the field of surface reactions on the powder particles, the formation of oxides and hydroxides, water films and their dependencies on alloy composition, temperatures, and atmospheric conditions. Progress in the research of powder particle reactions with the environment can be achieved with computational materials science techniques, for example, with density functional calculations of water adsorption on oxide layers [19] together with controlled laboratory experiments and advanced surface analysis techniques.

Beam–powder interactions: heating and melting

Once the powder is spread over the build plate, laser or electron beams interact with the powder beds. Laser-based machines are set up so that the beams directly melt the powder. For electron beam machines, an intermediate step is necessary to pre-sinter the powder particles. Without the pre-sintering, the powder particles would repel each other due to a beam-induced, negative charging. The pre-sintering ensures that the subsequent melting step does not cause a "smoking" of the powder bed, i.e., the repulsion of the particles over the entire build chamber. Typical beam sizes at the powder bed surface for commercial equipment range from below 30 micrometers for lasers in the 100 W range, to about 500 micrometers for lasers at powers of 200 W and up with typical sizes around 100 micrometers. It is often assumed that the intensity distribution across the laser beam follows a Gaussian profile, i.e., a maximum intensity at the beam axis that falls off in intensity radially following a Gaussian function. The beams scan over the powder beds at speeds on the order of meters per second and, depending on the beam control, the beam might scan the powder bed continuously or in a spot mode. The current beam sizes and powder size distributions imply that the beam "sees" at any time not more than about four particles at the surface and can roughly match the size of a single particle.

At laser powers of tens to about 1 kW, the beam penetrates the surface regions of the powder particles at a depth on the order of hundred nanometers [20–23]. At electron beam accelerating voltages of a few kW, the beam penetrates the powder particles at an approximately micrometer penetration level [20–23]. For metallic powders, a portion of the incoming energy is reflected and the reflection coefficient depends on the temperature, but reflection coefficients at the 90 percent level are not uncommon for metallic materials [24]. With energy deposition limited to a fraction of the powder bed thickness—and for laser beams even limited to a fraction of a powder particle diameter—the melting of the powder bed then has to take place from the top portions of the powder particles that transform into the liquid state toward the substrate. The heating of the powder particle regions that are directly exposed to the beams to their liquidus temperatures occurs in microseconds. The further melting of the powder bed from the top liquid layer to the previously melted layer that acts as a substrate then occurs as heat conduction through the powder bed. Hence, the melting process can be broken down into the initial surface melting step, followed by a heat conduction stage with energy being conducted from the top liquid layer of the powder bed to the powder particles underneath the liquid layer. The heat conduction in packed beds has received considerable attention (e.g., [25–30]), but in case of powder bed additive manufacturing, the powder bed does not remain static during the heating process. Instead, liquid alloy penetrates the powder beds from the top liquid layers. The thermal conduction through the powder bed, therefore, competes with the liquid alloy surrounding and melting the powder particles as the liquid penetrates the powder bed from the top surface layer to the previously melted and solidified layers [31]. The penetration of the powder bed is mainly driven by capillary forces. Gravitational forces are present, but can be neglected compared to the capillary forces. This can be seen from the capillarity constant, which equals $\sqrt{2\sigma/g\rho}$ where σ represents the surface tension, g the gravitational acceleration, and ρ the liquid density [32]. If the capillary constant exceeds a typical inter-particle spacing, then the gravitational forces can be neglected. For Ti-6Al-4V at its melting point, the surface tension is about 1.5 N/m [33] and the density is about 4.1×10^3 kg/m^3 [34]. The capillary constant is therefore on the order of one centimeter, but the spacing between powder particles used

for additive manufacturing is certainly much less than one centimeter, and hence, the gravitational forces can be neglected compared to capillary forces. The importance of capillary forces for the powder bed melting implies that surface energies of the liquid and solid alloys and liquid–solid interfacial energies are paramount to the melting process in powder bed additive manufacturing. The powder particle arrangement, particularly the effective packing density, forms the backdrop against the melt penetration, and the complete powder bed melting phenomenon is controlled by a combination of the particle arrangements and the capillary-driven melt penetration of the powder bed. Theoretical models have been developed for liquid penetration of porous structures that underscore the importance of surface energies and the melt propagation speed [35, 36]. Surface energies are difficult to determine experimentally, but progress in density functional theory offers an emerging alternative for obtaining surface energy data for some materials and surface orientations [37, 38]. The density functional theory calculations not only offer opportunities to obtain surface energies for some materials and surface orientations, but also for probing the effect that impurities have on surface energies [39] or for studying surface-gas reactions such as oxidation reactions [40]. The surface energies depend on temperature and composition, and for the latter, the dependence can be sensitive to minor alloy additions or impurities. The key objective of the melting step is to melt the entire powder bed and to reduce or eliminate the formation of voids and unmelts in the final parts. Unmelts are regions in the final additively manufactured components that are not entirely melted. While the reasons for unmelts and void formation require further investigations, gaps in the initial powder bed due to powder spreading anomalies could cause the formation of unmelts. Besides the surface energies of the liquids and solids, the wetting behavior of the liquid alloys on the solid powder particle surfaces is another important metallurgical aspect. Wetting describes the spreading of liquids on other phases, typically on solid surfaces and the angles that a liquid develops on a surface. These angles, and hence the wetting behavior, are determined by the surface energies of the solid, liquid, and vapor phases relative to each other, i.e., the surface energy of the solid in contact with the liquid, with the solid, and the liquid in contact with the vapor.

The sequence of melting on top of the powder bed and melt progression toward the previously melted layers implies that laser power changes do not directly affect the entire melting process. Instead, changes in laser power or speed only directly affect the surface regions of the powder particles that transform into liquid alloy. The melting of the top regions of the powder particles and the subsequent melt penetration into the powder bed represent a sequential process, and the slowest partial process, i.e., the melt progression into the powder bed, therefore determines the overall kinetics of the melt process. The melting of the surface powder particles requires a close beam control. If the temperature of the alloy increases well above the liquidus temperatures and approaching the boiling temperatures, challenges occur with alloy element evaporation. Elements differ in their saturated vapor pressure–temperature dependencies, and upon heating and melting, some alloy elements can evaporate from the melt preferentially. This phenomenon is known in the casting industry, and is addressed with modifications in the alloy compositions to end up with the correct alloy composition after the melting process. This practice can be expected to apply to additive manufacturing, but with the added difficulty that the exact temperature–time histories of the melt pools are very difficult to measure due to the beam speed and size; it is equally difficult to control the beam-induced heating so that the powder particles melt but without much overshoot in temperature above their liquidus temperatures. An additional complexity in the melting process is that depending on the powder storage and the material, the powder particles can be covered by thin oxide layers and adsorbed water films. If the oxide layer thicknesses are on the order of 100 nm, then the laser beam heating will take place mostly within the oxide layers, and due to specific heat capacity values that differ from those of the base metals and generally higher melting points of the oxide phases compared to the base metals, the laser beam settings required to melt the metal will differ from those of the oxide layers. This could induce temperatures in the metal much beyond the liquidus temperatures and, with an exponential dependence of the saturated vapor pressures on temperature, alloy composition changes could occur. The presence of oxide layers on the starting powder particles and of oxygen molecules in the build chambers furthermore suggests that oxide layers could form on the melt pool surfaces. But the laser or electron beams are likely to disrupt thin oxide layers and disperse the oxides in the melt pool. Moreover, as further described in the next paragraph, the melt pool is convective. Thin oxide layers on the melt pool surface would have to be affected by the convection of the melt pool. Since the surface of the melt pool is the boundary at which evaporation of atoms from the melt pool occurs and at which spatter leaves the melt pool as explained in the next paragraph, the effects of convection and oxide layers on the additive manufacturing require further studies. Table 1 summarizes process and material parameters and outcome quantities for the powder bed, the raking process, heating, and melting of the powder bed. It is very likely that additional process parameters and also material parameters will be identified as research progresses on powder raking and beam–powder interactions.

During the additive manufacturing process, sparks come off the impact regions of the beams on the powder beds. This phenomenon is known in welding applications, where

Table 1 Summary of process and material parameters and outcome quantities for powder bed raking, heating, and melting

	Process/material parameters	Relevant outcome quantities
Powder bed	Build plate surface characteristics	Powder bed uniformity: bed height and distribution of free space across the powder bed should be homogeneous across build plate
	Atmosphere in build chamber	Powder flow on build plate (repeatable amount of powder on build plate)
	Rake velocity	
	Rake design	
	Gap height	
	Particle size distribution	
	Powder surface chemistry	
Powder heating	Powder size distribution	Temperature–time profile across powder bed
	Powder surface chemistry	
	Powder composition	
	Thermal conductivity	
	Specific heat	
	Beam characteristics (power, speed, spatial intensity distribution, wavelength)	
Powder melting	Powder composition	Melt pool size and shape
	Surface tension	Melt pool reactions with build chamber atmosphere
	Powder (solid)-atmosphere interface energy	Regions of incomplete melting
	Powder (liquid)-atmosphere interface energy	Temperature distribution in and around melt pool
	Powder size distribution	Boundaries of melt pool (e.g., semi-molten particles attached to pool/powder bed interface
	Powder surface chemistry	Volume changes (solid–liquid, powder bed specific volume vs. liquid alloy specific volume vs bulk solid specific volume)
	Porosity, trapped gas in powder particles	Dynamics of gas pores, turning into bubbles inside the melt pool
	Beam characteristics (power, speed, spatial intensity distribution, wavelength)	
	Atmosphere in build chamber	

it is called "spattering" and refers to the ejection of small liquid metal droplets from the melt pool into the surrounding [41]. Two explanations currently exist for spatter formation during additive manufacturing. Metal vapors that evaporate from the melt pool surface exert a recoil pressure onto the melt pool that drives liquid alloy toward the edges of the melt pool or toward the center, depending on the surface flow pattern of the liquid [42]. If the recoil pressure onto the melt pool exceeds a threshold, small droplets might eject from the melt pool [43, 44]. The threshold pressure depends on the surface tension of the liquid alloy [43, 44]. This explanation resembles strongly the explanation for keyhole formation during laser or electron beam welding. Metal atoms evaporating from the weld pool exert a recoil pressure onto the weld pool surface. If the recoil pressure exceeds a critical value, the liquid alloy in the weld pool is ejected from the cavity that forms the weld pool. Depending on the beam speed and intensity, the ejection of the liquid alloy in the weld pool can cause a deepening well that is referred to as a 'keyhole' [45]. Another factor that is likely to play a role for spatter formation is gas pores or bubbles in the melt pool. Without direct experimental proof, it can be argued that these bubbles could originate from pores in the starting powder particles that are filled with inert gases in case of gas-atomized powders [46]. It is also possible that bubbles nucleate and grow due to supersaturations of gases such as hydrogen in the melt pool [47]. Upon melting, the gas in the powder particle pores might be released into the melt pool to form bubbles. The bubbles would follow the melt flow that is caused by convection within the melt pool and would be swept to the melt pool surface where bursting bubbles could contribute to the formation of spatter. Bubbles might also form when hydrogen gas is induced in the melt pool, for example, upon dissociation of water molecules and the solubility of hydrogen in the liquid alloy

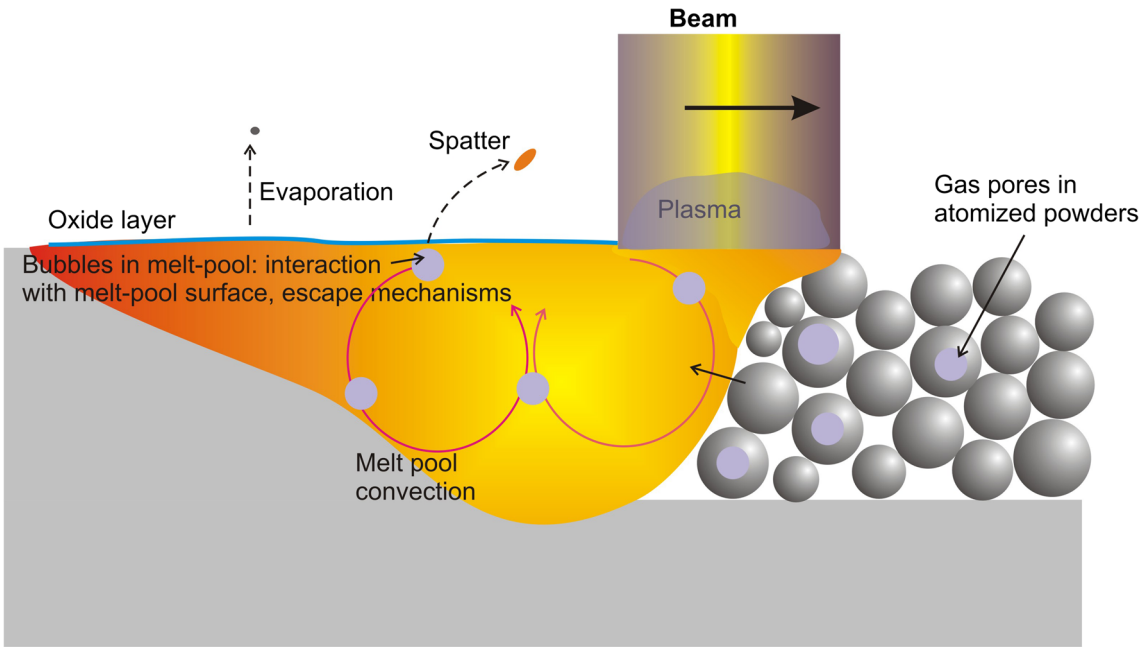

Fig. 2 Schematic illustration of melt pool phenomena during powder bed melting

decreases with temperature. The melt flow in the melt pool is caused by the temperature dependence of the surface tension and the melt density. Depending on the sign of the surface tension temperature gradient, liquid alloy is either pulled toward the hottest regions on the melt pool surface or is pulled away from the hottest to the colder regions. Similarly, density decreases with increasing temperature induce a vertical motion of the melt in the melt pool. The combination of surface, horizontal melt motion, and vertical motion can induce convection patterns that are often referred to as Marangoni convection [48]. The formation of bubbles in melt pools and ensuing porosity is not very well characterized for welding, but much less so for additive manufacturing. The bubble/porosity aspect shows similarities between welding research and additive manufacturing research, and results from welding research in this case appear useful for an understanding of porosity formation during additive manufacturing.

With laser or electron beam sizes of about 100 micrometers and beam speeds on the order of 1 m/s, the heating rate of the powder bed can be estimated. The beams spend on the order of 10^{-4} s on a surface patch with a size of the beam, i.e., 100 micrometers. During that time of 10^{-4} s, the powder bed has to reach the liquidus temperature, and therefore, depending on the specific values of the liquidus temperatures, the heating rates can be estimated and are approximately on the order of 10^{7} K/s for liquidus temperatures on the order of 1000 K. Rapid heating can modify the phase formation and phase transformation behavior. For example, pulsed-laser processing experiments with pure Manganese demonstrated that due to the rapid heating, the transformation from alpha-Mn that is stable at room temperature to the other allotropes was suppressed, and therefore, the alpha-Mn melted at its melting point, which represents an undercooling relative to the equilibrium melting point of Mn [49]. In nucleation-controlled phase transformations, rapid heating requires modifications of the classical nucleation theory [50]. In case of current additive manufacturing, the alloy powder particles are synthesized with rapid quenching technologies and can reveal non-equilibrium microstructures and phases that add to the complexity of the laser or electron beam-induced rapid heating of the powder bed. The brief overview of physical phenomena that are highlighted schematically in Fig. 2 occurring during the heating and melting of powder beds shows the complexity of the process and the resulting challenges in a complete model of powder bed heating and melting. Besides the difficulties in understanding each phenomenon individually, interactions are expected, for example, the interaction of bubbles with the melt pool surface in the presence of oxide skins on the melt pool. These interactions add to the challenges understanding the additive manufacturing process.

Powder bed solidification

With the formation of a melt pool during the powder bed heating, the physical mechanisms reach more familiar grounds than for the powder bed heating stage. Once a melt pool has formed, the subsequent solidification of the liquid

phase follows theories and models that are at least in general established and known. Still, a few aspects of the solidification process set powder bed additive manufacturing apart from traditional castings. The melt pool size is only on the order of hundreds of micrometers to millimeters for additive manufacturing, regardless of the size of the final component, and therefore quite different from castings with much larger melt pool sizes. The small melt pool size implies that macrosegregation is limited in contrast to large-size castings. In lateral directions, the powder beds surrounding the melt pools exhibit thermal conductivities that are significantly less than the same alloys in bulk form. For example, the thermal conductivity of alumina is between about 25 and 30 W/m * K [51], while that of alumina powder beds was reported to be about 0.3 W/m * K at near ambient temperatures [52], and therefore, conductive heat transfer occurs mostly into the previously melted layers underneath the melt pools. Finally, and maybe most significantly, the cooling rates of the melt pools during additive manufacturing reach values that have been estimated to be between hundreds of Kelvin per second [53] to about 10^3 K/s. At these cooling rates, deviations from near-equilibrium freezing conditions are expected that have received much research interest in the rapid solidification community [54–56]. Different levels of equilibrium exist in materials [57], and the cooling rates associated with additive manufacturing suggest deviations from global equilibrium. Even at cooling rates encountered during melt-spinning with typical cooling rates estimated to be on the order of 10^5–10^6 K/s [55], it is generally assumed that local interfacial equilibrium is maintained. Therefore, the same assumption should be made for the additive manufacturing process. In general, the rapid cooling conditions during additive manufacturing should impact additively manufactured parts potentially in several different ways. Characteristic sizes of microstructural features such as grains, lamellae, or second phase particles typically decrease under rapid cooling conditions compared to conditions found in standard casting operations [58]. Another potential outcome of rapid cooling conditions is that dendritic segregation is mitigated to the point where near compositional homogeneity can be achieved for the highest experimentally achievable cooling rates [58]. Under rapid cooling conditions, some phases that would develop under conditions of global equilibrium might not form, giving way to the occurrence of metastable phases. The nature of the metastable phases depends on the alloy composition and the thermal history of the quenching process. This aspect is highlighted schematically in Fig. 3. For cooling rate $\dot{T}1$, the primary phase to nucleate is phase I. For the higher cooling rate $\dot{T}2$, the nucleation of phase I is bypassed and phase II nucleates. A related scenario is highlighted in Fig. 4. The hypothetical phase diagram in Fig. 4 shows a delta phase for the equilibrium condition. But if the delta phase cannot form during quenching from the liquid state, a simple eutectic system might form as highlighted with the dashed phase boundaries. This metastable phase diagram reveals characteristics that differ from the equilibrium phase diagram; in the hypothetical case shown in Fig. 4, the eutectic temperature is reduced and the eutectic composition differs from the equilibrium phase diagram.

A unique aspect of electron beam-based additive manufacturing from a rapid cooling perspective is the elevated build temperature during the process. The electron beam is used to maintain temperatures of several hundreds of degrees Celsius during the build process. The rapid cooling

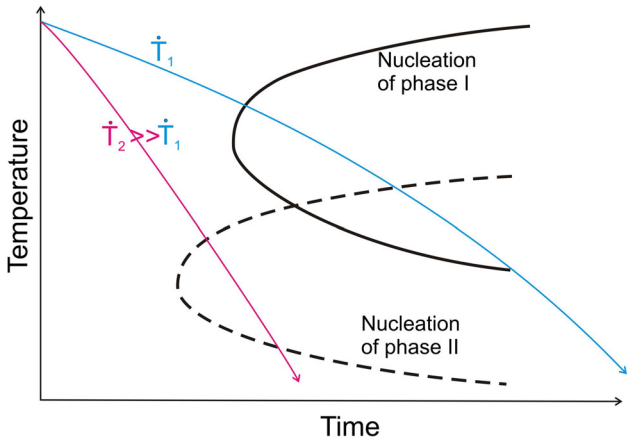

Fig. 3 Time–temperature diagram showing the nucleation onset for two different hypothetical phases and two different cooling rates (*dashed lines*). The nucleation of phase I is bypassed at the higher cooling rate of the two, $\dot{T}2$

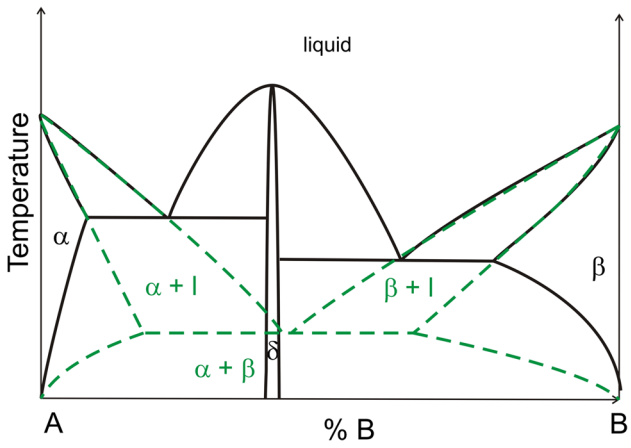

Fig. 4 Hypothetical equilibrium phase diagram (*solid lines*) and metastable phase diagram (*dashed lines*)

conditions, therefore, occur at the liquid–solid transition, but the melt pool is effectively quenched into a high-temperature thermal reservoir. The rapid cooling to high temperatures in the solid state represents an additional option for microstructure and phase formation control. The thermal arrest at high temperatures in the solid state could prevent some metastable phases from forming that would develop if the sample would cool to room temperature. The exposure to high temperatures, typically for hours if not days, in the additive manufacturing equipment effectively represents a heat treatment. If metastable phases would develop during the rapid solidification process, phase transformation might occur or the quenched-in microstructure could respond, for example, with grain-growth or coarsening reactions. The deviations from equilibrium pertain to microstructures and phase formation [58, 59]. Current efforts in additive manufacturing focus on common engineering alloys such as Ti-6Al-4 V or IN718 with the aim to achieve properties according to specifications. These alloys were developed for processing techniques with significantly different time–temperature process characteristics, and opportunities abound to modify alloys or develop new alloys with the additive manufacturing processing characteristics in mind.

From a practical viewpoint of build completion, the interior of the additive manufacturing machines reaches temperatures of about 80 °C for laser machines without active heating, but in case of electron beam machines, the entire build block, consisting of pre-sintered powder and components, is heated by the beam to elevated temperatures of several hundreds of degrees Celsius. When the build process is complete, the block of pre-sintered powder, including the embedded components, cools off at cooling rates that prevent residual stresses from building up. For laser-based machines, since the temperatures of the components during the build process are close to ambient temperatures, significant residual stresses build up [60–64]. The residual stresses are caused mainly by the volume decrease during the liquid to solid transformation of most metals and the volume decrease in the solid state during cooling. The two key properties of materials that are relevant for the buildup of residual stresses are the specific volume change during freezing and the thermal expansion behavior. In addition to the material properties, the residual stress buildup depends on the laser beam pattern, sample geometry and layout in the build chamber, and the build plate [64]. The residual stresses require support structures for the parts to be additively manufactured. These support structures anchor the parts to the build plates. The support structure aspect of additive manufacturing is an important topic, but falls outside the domain of metallurgical aspects of the additive manufacturing process.

Post-processing

Once the build plates with attached components are removed from the additive manufacturing machines, post-processing operations need to be applied. Powder removal for laser-additively manufactured parts is achieved with brushing or compressed air. For electron beam machines, due to the pre-sintering step, a simple brushing off of powders is insufficient to recover the components. Instead, powder recovery systems are used that are essentially sand-blasting machines except that the same powder material is used for the blasting operation as for the original parts in the additive manufacturing machines. Powder removal is particularly important for interior passages that cannot be accessed easily with the grit-blasting approach. Among removal techniques in different development stages, the chemical etching away of powder in passages could require metallurgical studies of interior passage surface behavior. From a metallurgical viewpoint, the heat-treating and surface finish operations require attention. Stress-relief heat-treating, aging treatments, and hot-isostatic pressing [65] are necessary post-processing operations for most additive manufacturing applications. Heat treatment procedures will require modifications for most alloys to achieve mechanical property specifications. The heat-treating modifications depend on the alloy and the additive manufacturing details, and a general, brief summary of the specific adjustments of the heat treatment specifications and procedures is beyond the scope of this article. There are additional aspects unique to additive manufacturing that offer a wider array of microstructure control opportunities than those available to engineering alloys processed with conventional manufacturing technologies. For example, the residual stresses that develop during laser-based powder bed additive manufacturing should help alleviate some of the microstructure features that develop during the additive manufacturing process. Elongated grains are often observed in as-built microstructures [66, 67], and the residual stresses could promote the formation of equiaxed grains during heat treatment-induced recrystallization reactions.

Summary

There is a great need to understand all mechanisms that control metal additive manufacturing. This need arises from current challenges with the qualification of additively manufactured parts. A knowledge of the mechanisms underlying additive manufacturing helps predict the effects of material- and process parameters on part properties and the variations in material- and process parameters on variations in part properties. In the long term, the knowledge of additive manufacturing mechanisms will be used to

improve processes and materials. Metallurgy plays a central role in contributing to a complete understanding of metal additive manufacturing. The sequence from powder storage, to spreading in the machines, to melting, solidification, and post-processing encompasses several metallurgy topics. Surface reactions such as oxidation and water vapor absorption affect the powder flow and melting behavior. Thermophysical properties, including surface energies, liquidus temperatures, thermal conduction, and specific heats, determine the heating and melting behavior of powder beds alongside the machine parameters. Heating rates are estimated to be on the order of 10^6–10^7 K/s, and cooling rates are on the order of several hundreds of degrees per second. These high heating and cooling rates shift microstructure evolutions and phase selections strongly toward non-equilibrium with implications on grain-sizes and morphologies and the formation of metastable phases. The deviations in microstructures from conventionally processed alloys require heat treatments to be modified to achieve the properties required for existing engineering alloys. The breadth of metallurgical topics and their nature suggest that only a combination of theoretical, experimental, and computational approaches can succeed in yielding the necessary results. For example, some thermophysical properties can be measured directly, while other properties, for example, surface energies, are amenable to first principles calculations. The level of relevance of some metallurgical topics is not known at this point, but the interactions of powder particles in the powder beds with liquid alloys of the same composition and rapid solidification aspects should play a central role as additive manufacturing research moves forward.

Compliance with ethical standards

Conflict of Interest The author declares that he has no conflict of interest.

References

1. Frazier WE (2014) Metal additive manufacturing: a review. J Mater Eng Perform 23:1917–1928
2. Bertrand P, Bayle F, Combe C, Gœuriot P, Smurov I (2007) Ceramic components manufacturing by selective laser sintering. Appl Surf Sci 254:989–992
3. Gockel J, Beuth J (2013) Understanding Ti-6Al-4V microstructure control in additive manufacturing via process maps. Solid Freeform Fabr Proc Austin, TX Aug:666–675
4. Gaskell DR (2008) Introduction to the thermodynamics of materials. CRC Press, Boca Raton
5. Ellingham HJT (1944) Reducibility of oxides and sulphides in metallurgical processes. J Soc Chem Ind L 63:125–160
6. Kubaschewski O, Hopkins BE (1962) Oxidation of metals and alloys. Butterworths, London
7. Birks N, Meier G, Pettit F (2009) Introduction to the high temperature oxidation of metals. Cambridge University Press, Cambridge
8. Henderson MA (2002) The interaction of water with solid surfaces: fundamental aspects revisited. Surf Sci Rep 46:1–308
9. Hodgson A, Haq S (2009) Water adsorption and the wetting of metal surfaces. Surf Sci Rep 64:381–451
10. Matei G, Claussen N, Hausner HH (1974) Influence of relative humidity on flow behavior of metal and ceramic powders. Mod Dev Powder Met 8:5–11
11. Mohandas T, Banerjee D, Kutumba Rao VV (1999) Fusion zone microstructure and porosity in electron beam welds of an alpha plus beta titanium alloy. Metall Mater Trans A 30A:789–798
12. Gouret N, Dour G, Miguet B, Ollivier E, Fortunier R (2004) Assessment of the origin of porosity in electron-beam-welded TA6V plates. Metall Mater Trans A 35A:879–889
13. Karde V, Panda S, Ghoroi C (2015) Surface modification to improve powder bulk behavior under humid conditions. Powder Tech 278:181–188
14. Kwek JW, Ng WK, Tan CL, Chow PS, Tan RBH (2006) The effects of particle surface properties and storage condition on powder flow properties. In: AIChE Spring national meeting—5th world congress on particle technology, April 23, 2006–April 27, 2006, Orlando
15. Liew WYH (2006) The effect of relative humidity on the unlubricated wear of metals. Wear 260(7–8):720–727
16. Hogg R (2009) Mixing and segregation in powders: evaluation, mechanisms and processes. KONA Powder Part J 27:3–17
17. Metcalfe G, Shattuck M (1996) Pattern formation during mixing and segregation of flowing granular material. Phys A 233:709–717
18. Slotwinski JA, Garboczi EJ, Stutzman PE, Ferraris CF, Watson SS, Peltz MA (2014) Characterization of metal powders used for additive manufacturing. J Res NIST 119:460–493
19. Zhang C, Lindan PJ (2004) A density functional theory study of the coadsorption of water and oxygen on TiO_2(110). J Chem Phys 121(8):3811–3815
20. Von Allmen MF (1982) Fundamentals of energy deposition. In: Poate JM, Mayer JW (eds) Laser annealing of semiconductors. Academic Press, London, pp 43–74
21. Von Allmen MF, Blatter A (1994) Laser-beam interactions with materials. Springer, Berlin
22. White CW, Peercy PS (1980) Laser and electron beam processing of materials. Academic Press, New-York
23. White CW, Aziz MJ (1987) Energy deposition, heat flow, and rapid solidification during pulsed-laser and electron-beam irradiation of materials. In: Rehn LE, Picraux ST, Wiedersich H (eds) Surface alloying by ion, electron, and laser beams. American Society of Metals, Metals Park, OH, pp 19–51
24. Ready JF (1978) Industrial applications of lasers. Academic Press, New-York
25. Slavin AJ, Arcas V, Greenhalgh CA, Irvine ER, Marshall DB (2002) Theoretical model for the thermal conductivity of a packed bed of solid spheroids in the presence of a static gas with no adjustable parameters except pressure and temperature. Int J Heat Mass Tran 45:4151–4161
26. Schertz WW, Bischoff K (1969) Thermal and material transport in nonisothermal packed beds. AIChE J 15:597–604
27. Bahrami M, Yovanovich MM, Culham JR (2006) Effective thermal conductivity of rough spherical packed beds. Int J Heat Mass Tran 49:3691–3701
28. Shapiro M, Dudko V, Royzen V, Krichevets Y, Lekhtmakher S, Grozubinsky V, Shapira M, Brill M (2004) Characterization of powder beds by thermal conductivity: effect of gas pressure on the thermal resistance of particle contact points. Part Part Syst Charact 21:268–275

29. Huethorst JAM, Leenaars AFM (1990) A new model for the effective thermal conductivity of packed beds of solid spheroids alumina in helium. Colloid Surface A 50:101–111
30. Kikuchi S (2001) Numerical analysis model for thermal conductivities of packed beds with high solid to gas conductivity ratio. Int J Heat Mass Trans 44:1213–1221
31. Körner C, Bauereiss A, Attar E (2013) Fundamental consolidation mechanisms during selective beam melting of powders. Model Simul Mater Sc 21:1–18
32. Landau LE, Lifshitz EM (1959) Chapter VII—surface phenomena. In: Fluid mechanics, vol 6 of a theoretical course in physics. Pergamon-Press Ltd., London, pp 230–232
33. Wunderlich R (2008) Surface tension and viscosity of industrial Ti-alloys measured by the oscillating drop method. High Temp Mater Processes (London) 27(6):401–412
34. Li JJZ, Johnson WL, Rhim W-K (2006) Thermodynamic expansion of Ti-6Al-4V measured by electrostatic levitation. Apply Phys Lett 89:111913–111917
35. Denesuk M, Smith GL, Zelinski BJJ, Kreidl NJ, Uhlman DR (1993) Capillary penetration of liquids into porous materials. J Colloid Interf Sci 158:114–120
36. Lavi B, Marmur A (2006) The capillary race: optimal surface tensions for fastest penetration. Colloids Surf A Physicochem Eng Asp 282–283:263–271
37. Singh-Miller NE, Marzari N (2009) Surface energies, work functions, and surface relaxations of low-index metallic surfaces from first principles. Phys Rev B 80(23):235407–235416
38. Hafner J (2008) Ab-initio simulations of materials using VASP: density-functional theory and beyond. J Comput Chem 29(13):82–116
39. Sharma V, Alpay P (in preparation)
40. Reuter K, Scheffler M (2004) Oxide formation at the surface of late 4d transition metals: insights from first-principles atomistic thermodynamics. Appl Phys A 78(6):793–798
41. Nakamura H, Kawahito Y, Nishimoto K, Katayama S (2015) Elucidation of melt flows and spatter formation mechanisms during high power laser welding of pure titanium. J Laser Appl 27:032012-032011
42. Bäuerle D (2000) Laser processing and chemistry. Springer, Berlin
43. Simonelli M, Tuck C, Aboulkhair N, Maskery I, Ashcroft I, Wildman R, Hague R (2015) A study on the laser spatter and the oxidation reactions during selective laser melting of 316L stainless steel, Al-Si10-Mg, and Ti-6Al-4V. Metall and Mat Trans A 46:3842–3851
44. Rabin BH, Smolik GR, Korth GE (1990) Characterization of entrapped gases in rapidly solidified powders. Mater Sci Eng A A124:1–7
45. Matsunawa A, Kim J-D, Seto N, Mizutani M, Katayama S (1998) Dynamics of keyhole and molten pool in laser welding. J Laser Appl 10:247–252
46. Ng GKL, Jarfors AEW, Bi G, Zheng HY (2009) Porosity formation and gas bubble retention in laser metal deposition. Appl Phys A 97:641–649
47. Huang JL, Warnken N, Gebelin J-M, Strangwood M, Reed RC (2012) On the mechanism of porosity formation during welding of titanium alloys. Acta Mater 60:3215–3225
48. Kou S (2002) Welding Metallurgy, 2nd edn. Wiley Interscience, New-York, NY
49. Follstaedt DM, Peercy PS, Perepezko JH (1986) Phase selection during pulsed laser annealing of manganese. Appl Phys Lett 48:338–340
50. Shneidman VA, Weinberg MC (1996) Crystallization of rapidly heated amorphous metals. J Non-Cryst Solids 194:145–154
51. CES Edupack 2014. Granta
52. Sih SS, Barlow JW (2004) The prediction of the emissivity and thermal conductivity of powder beds. Particul Sci Technol 22:427–440
53. Brice C, Dennis N (2015) Cooling rate determination in additively manufactured aluminum alloy 2219. Met Mater Trans A 46A:2304–2308
54. Liebermann HH (ed) (1993) Rapidly solidified alloys. Marcel Dekker, New-York
55. Starke E Jr, Fine ME (eds) (1986) Rapidly solidified powder aluminum alloys. ASTM, West Conshohocken
56. International Conference on Rapidly Quenched and Metastable Materials. Triannial conference series since 1970
57. Boettinger WJ, Perepezko JH (1993) Fundamentals of solidification at high rates. In: Liebermann HH (ed) Rapidly solidified alloys. Marcel Dekker, New-York
58. Cantor B, Kim WP, Bewlay BP, Gillen AG (1991) Microstructure-cooling rate correlations in melt-spun alloys. J Mater Sci 26:1266–1276
59. Perepezko JH, LeBeau SE (1982) Nucleation of Al during solidification. In: Pampillo CA, Biloni H, Mondolfo L, Sacchi F (eds) Aluminum Transformation Technology and its Application. ASM, Metals Park, OH, pp 309–346
60. Casavola C, Campanelli SL, Pappalettere C (2009) Preliminary investigation on distribution of residual stress generated by the selective laser melting process. J Strain Anal Eng 44:93–104
61. Mercelis P, Kruth JP (2006) Residual stresses in selective laser sintering and selective laser melting. Rapid Prototyping J 12:254–265
62. Parry L, Ashcroft I, Bracket D, Wildman RD (2015) Investigation of residual stresses in selective laser melting. Trans Tech Publ 627:129–132
63. Yadroitsev I, Yadroitsava I (2015) Evaluation of residual stress in stainless steel 316L and Ti6Al4V samples produced by selective laser melting. Virtual Phys Prototyp. doi:10.1080/17452759.2015.1026045
64. Zaeh MF, Branner G (2010) Investigations on residual stresses and deformations in selective laser melting. Prod Eng 4:35–45
65. Bocanergra-Bernal MH (2004) Review hot isostatic pressing (HIP) technology and its applications to metals and ceramics. J Mater Sci 39:6399–6420
66. Murr LE (2015) Metallurgy of additive manufacturing: examples from electron-beam melting. Addit Manuf 5:40–53
67. Liu F, Lin X, Yang G, Song M, Chen J, Huang W (2011) Microstructure and residual stress of laser rapid formed Inconel 718 nickel-base superalloy. Opt Laser Technol 43:208–213